



HAL
open science

Multiple two-step oscillation regimes produced by the alto saxophone

Tom Colinot, Philippe Guillemain, Christophe Vergez, Jean-Baptiste Doc,
Patrick Sanchez

► **To cite this version:**

Tom Colinot, Philippe Guillemain, Christophe Vergez, Jean-Baptiste Doc, Patrick Sanchez. Multiple two-step oscillation regimes produced by the alto saxophone. *Journal of the Acoustical Society of America*, 2020, 147 (4), pp.2406-2413. 10.1121/10.0001109 . hal-02549931

HAL Id: hal-02549931

<https://hal.science/hal-02549931>

Submitted on 21 Apr 2020

HAL is a multi-disciplinary open access archive for the deposit and dissemination of scientific research documents, whether they are published or not. The documents may come from teaching and research institutions in France or abroad, or from public or private research centers.

L'archive ouverte pluridisciplinaire **HAL**, est destinée au dépôt et à la diffusion de documents scientifiques de niveau recherche, publiés ou non, émanant des établissements d'enseignement et de recherche français ou étrangers, des laboratoires publics ou privés.

Multiple two-step oscillation regimes produced by the alto saxophone

Tom Colinot,^{1, a)} Philippe Guillemain,¹ Christophe Vergez,¹ Jean-Baptiste Doc,² and
Patrick Sanchez¹

¹*Aix Marseille Univ, CNRS, Centrale Marseille, LMA, Marseille,
France*

²*Laboratoire de Mécanique des Structures et des Systèmes couplés,
Conservatoire National
des Arts et Métiers, Paris, France*

(Dated: 27 March 2020)

1 A saxophone mouthpiece fitted with sensors is used to observe the oscillation of
2 a saxophone reed, as well as the internal acoustic pressure, allowing to identify
3 qualitatively different oscillating regimes. In addition to the standard two-step
4 regime, where the reed channel successively opens and closes once during an
5 oscillation cycle, the experimental results show regimes featuring two closures of
6 the reed channel per cycle, as well as inverted regimes, where the reed closure
7 episode is longer than the open episode. These regimes are well-known on bowed
8 string instruments and some were already described on the Uilleann pipes. A simple
9 saxophone model using a measured input impedance is studied with the harmonic
10 balance method, and is shown to reproduce the same two-step regimes. The
11 experiment shows qualitative agreement with the simulation: in both cases, the
12 various regimes appear in the same order as the blowing pressure is increased. Similar
13 results are obtained with other values of the reed opening control parameter, as well
14 as another fingering.

^{a)} colinot@lma.cnrs-mrs.fr

15 **I. INTRODUCTION**

16 Various oscillating regimes, defined as the pattern of oscillations both mechanical and
17 acoustical that correspond to the production of a periodic sound, have been observed and
18 classified on bowed string instruments(Schelleng, 1973). The strongly non-linear friction law
19 between bow and string leads to an oscillation pattern known as stick-slip motion, where
20 the string sticks to the bow for a part of the period and then slips for another part of the
21 period. The stick-slip phases may occur twice per period, leading to the so-called “double
22 stick-slip” motion.

23 Reed conical instruments have often been compared to bowed strings, by virtue of the
24 cylindrical saxophone approximation, which replaces the conical resonator with two parallel
25 cylinders (Ollivier *et al.*, 2004) because their impedance is similar in low frequency. In
26 reed instruments, the analogous motion to stick-slip is called two-step motion (Ollivier
27 *et al.*, 2005). It consists in a beating reed regime, where the reed channel is closed for
28 part of the period, and open for the rest of the period. The most common case, where
29 the reed closure episode is shorter than half the period, is called standard two-step motion.
30 Otherwise, the regime is called inverted. Standard and inverted two-step motions have
31 been observed experimentally on a saxophone and predicted analytically on a cylindrical
32 equivalent (Dalmont *et al.*, 2000). Oscillating regimes showing more than one closure of
33 the reed per period were never studied on the saxophone to our knowledge. They have
34 been observed on a double reed instrument, the Irish Uilleann pipes (Dalmont and Le Vey,
35 2014). To observe the signals produced by a wind instrument in playing situation, with a

36 musician, an instrumented mouthpiece fitted with a reed displacement and pressure sensors
37 can be used. Instrumented mouthpieces can help explain features of the produced sound, for
38 instance spectral content on a saxophone (Guillemain *et al.*, 2010) or transient descriptors
39 on a clarinet (Pàmies-Vilà *et al.*, 2018). They also provide a means to estimate some
40 of the parameters of a physical model based on the dynamical behavior of the system
41 (Muñoz Arancón *et al.*, 2016).

42 This paper reports experiments in playing conditions exhibiting classic standard and
43 inverted regimes, as well as double two-step motions, where the reed channel closes twice
44 per period. To complete the study, we show that a simple saxophone model based on the
45 input impedance of the saxophone used for the experiment is able to reproduce these double
46 two-step regimes. The Harmonic Balance Method associated with continuation (Asymptotic
47 Numerical Method) is used to obtain periodic signals corresponding to several control
48 parameter combinations. The numerical simulations, in addition to experimental data,
49 provide insights about the possible ways of transition between single and double two-step
50 regimes, as well as the second register of the instrument. We also show that similar behavior
51 occurs for neighboring fingerings and control parameter values. Describing and categorizing
52 the oscillation regimes of the saxophone, as well as the musician's actions needed to obtain
53 them, is among the first steps towards objective characterization of the ease of playing of
54 an instrument.

55 II. EXPERIMENTAL OBSERVATION OF DOUBLE TWO-STEP MOTIONS ON 56 A SAXOPHONE

57 A. Experimental apparatus

58 An instrumented mouthpiece is used to monitor the blowing pressure, the pressure inside
59 the mouthpiece, and the position of the reed. It is shown in figure 1. It consists in a
60 modified saxophone mouthpiece (Buffet-Crampon) incorporating two pressure probes: one
61 going into the mouth of the musician and one into the mouthpiece, as well as an optical
62 sensor (Everlight ITR8307) measuring the displacement of the reed. The pressure probe
63 tubes are connected to a Honeywell TSCDRRN005PDUCV pressure sensor. The tubes have
64 a radius of 0.55 mm and a length of 20 mm (mouth pressure) and 62 mm (pressure in the
65 mouthpiece). According to (Guillemain *et al.*, 2010), the transfer function of these capillary
66 tubes is well represented by a model with non-isothermal boundary conditions (Keefe, 1984).
67 An inverse filtering was performed on the pressure signals to compensate the effect of the
68 probe tubes. Signals are then acquired using an NI USB-9234 card by National Instruments
69 at a 51.2 kHz sampling rate. Experimental signals displayed hereafter are not scaled or
70 converted as this work focuses on qualitative study of the regime types. The instrumented
71 mouthpiece is equipped with a saxophone reed (Rico Royal strength 2) and mounted on a
72 commercial alto saxophone (Buffet-Crampon Senzo).

73 Throughout the remainder of the paper, a low B fingering (written pitch) is studied. In
74 concert pitch, the fundamental note expected with this fingering is a $D3$ at the frequency
75 146.83 Hz. The input impedance of the saxophone for this fingering has been measured

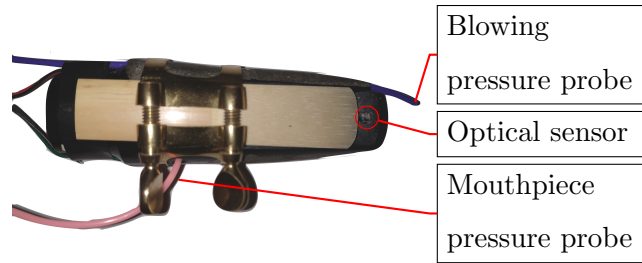


FIG. 1. Instrumented alto saxophone mouthpiece including pressure probes for the pressure in the mouth of the musician and in the mouthpiece, and an optical sensor measuring the displacement of the reed. The reed is pulled back so that the optical sensor is uncovered.

76 using the CTTM impedance sensor ([Dalmont and Le Roux, 2008](#)). Its modulus is displayed
 77 in figure 2. The B fingering, which produces the second lowest note on the instrument, is
 78 chosen because the double two-step regimes studied in this work tend to appear more easily
 79 on the lowest notes of the saxophone. Note that for this fingering, the note most commonly
 80 expected by musicians is the first register, whose frequency is around the first impedance
 81 peak. On this fingering, the first register is often hard to produce, especially for beginner
 82 musicians. This can be understood when looking at the impedance modulus curve on figure 2,
 83 where the first peak is lower than the next three peaks: the upper resonances of the bore play
 84 a large part in the sound production, leading to a complicated sound production behavior.
 85 This profile of amplitude of the first few impedance peaks is also found in soprano and tenor
 86 saxophone ([Chen et al., 2009](#)). The lowest fingering ($B\flat$) was not chosen, although it was
 87 tested, because it is more subject to producing undesired multiphonics and quasi-periodic
 88 regimes.

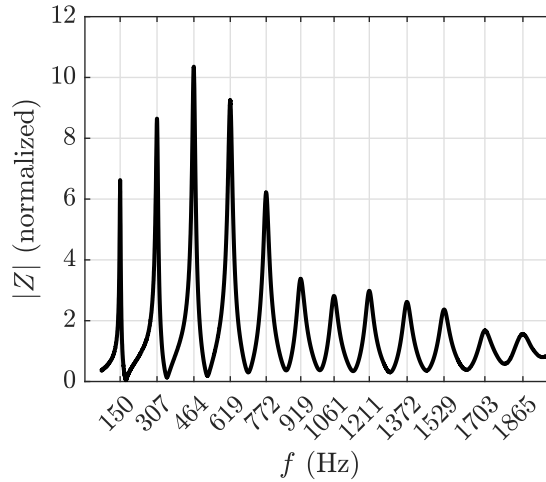


FIG. 2. Input impedance modulus measured for the studied fingering of the alto saxophone: low B in written pitch. The modulus of the impedance is normalized by the characteristic impedance at the input of the instrument.

89 B. Observation of single and double two-step oscillating regimes

90 The main oscillating regimes of a saxophone are beating, which means that the reed
 91 channel closes completely during part of the cycle. They can be thought of as two-step
 92 motions (Ollivier *et al.*, 2004) and classified as standard or inverted, depending on the
 93 relative duration of the open and closed episode. Different regimes can be obtained for the
 94 same fingering, just by varying the control parameters such as the blowing pressure. Figure
 95 3 shows measured examples of these two-step regimes. The reed displacement signal was
 96 post-processed by subtracting its moving average over a period, to be centered around 0.
 97 The standard regime is characterized by an open episode and a short closed episode. As
 98 can be seen on figure 3 (a), the reed is opened – and displays small amplitude oscillations
 99 around the highest values of x – for about 6 ms. Its closure corresponds to the main dip in

100 the waveform and it lasts for about 1 ms per period. For the inverted motion on figure 3
 101 (b), the duration ratio is reversed: the reed channel is almost at its narrowest about 6 ms
 102 and opens wide briefly for about 1 ms. Note that the standard regime is obtained for lower
 103 values of the blowing pressure than the inverted regime.

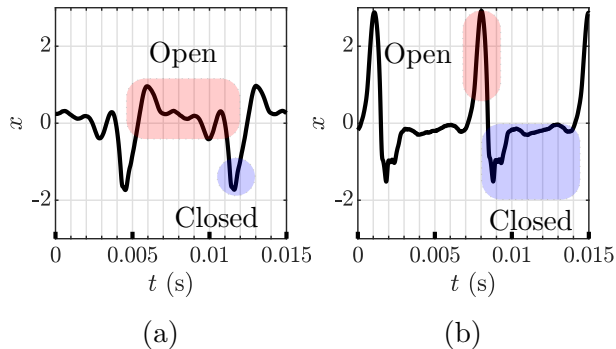


FIG. 3. Measured reed position for simple two-step motions: standard (a) and inverted (b). The reed channel is closed when x is low. These waveforms correspond to different blowing pressures (see circle markers on figure 5).

104 The analogy with bowed string instruments suggests the apparition of other types of
 105 regimes. For example, under given excitation condition, bowed strings are subject to the
 106 double stick-slip phenomenon (Woodhouse, 2014), an oscillation regime where the string slips
 107 under the bow twice per period (instead of once for the standard Helmholtz motion). When
 108 transposed to conical reed instruments, this phenomenon corresponds to two closures of the
 109 reed channel per period. These regimes are observed experimentally on the low fingerings of
 110 the saxophone and they can be standard or inverted, as shown in figure 4. This oscillating
 111 regime can be called “double two-step”. Note that the double two-step regime is distinct
 112 from second register regimes: it is a first register regime, as it produces the same note as

113 the standard two-step regime. For the standard version of the double two-step regime, the
114 closure episodes are about 1 ms, almost the same duration as in the single standard two-step
115 motion (figure 3, (a)). For the inverted double two-step regime, the short openings of the
116 reed channel also last for about 1 ms. For illustration purposes, the audible sound outside
117 the instrument was recorded and short clips are provided as multimedia files 3, 4, 1 and 2.
118 Note that the audible sound corresponding to these double two-step regimes (Mm. 3 and
119 4) is clearly different from single regimes (Mm. 1 and 2). The difference in audible sound is
120 less clear between a standard regime and its inverted counterpart.

121 [Mm. 1](#). Sound recorded outside the resonator for the standard two-step motion, corresponding
122 to the measured displacement shown in figure 3, (a).

123 [Mm. 2](#). Sound recorded outside the resonator for the inverted two-step motion, corresponding
124 to the measured displacement shown in figure 3, (b).

125 [Mm. 3](#). Sound recorded outside the resonator for the double two-step motion, corresponding
126 to the measured displacement shown in figure 4, (a).

127 [Mm. 4](#). Sound recorded outside the resonator for the inverted double two-step motion,
128 corresponding to the measured displacement shown in figure 4, (b).

129 In order to estimate the relative regions of production of each kind of regime in the
130 control parameter space, a blowing pressure ramp is performed by a musician and recorded
131 using an instrumented mouthpiece for the B fingering of the test saxophone. The musician

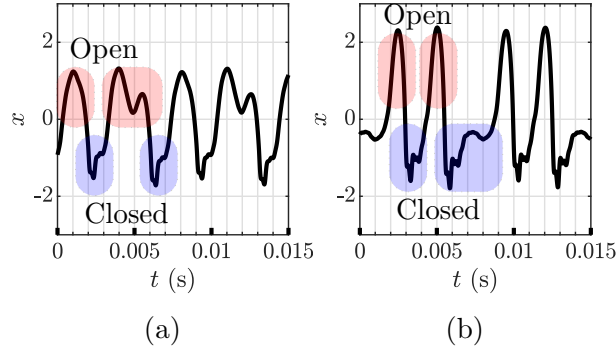


FIG. 4. Measured reed position for double two-step motions: standard (a) and inverted (b). These waveforms correspond to different blowing pressures (see circle markers on figure 5).

132 sees the evolution of the blowing pressure parameter in real-time on a screen. The player
 133 makes as little embouchure adjustments as possible and focuses on increasing the blowing
 134 pressure progressively. Results are shown in figure 5. This ramp was obtained in a single
 135 breath after several tries. For clarity, the blowing pressure signal is smoothed by a moving
 136 average with a rectangular window, adjusted to reject the fundamental frequency of the
 137 oscillations and keep only the slowly varying value of the signal. Regimes are classified
 138 automatically based on the ratio of duration of the open and closed reed episodes. The reed
 139 displacement signal is high-pass filtered in order to remove the DC component. The reed
 140 is then considered “open” when the displacement signal is above 0 and “closed” when it is
 141 below 0. The ratio between closed duration and oscillation period is then computed and
 142 averaged over 4 periods. Thresholds are defined arbitrarily to separate between the different
 143 types of regimes, at 0.1, 0.25, 0.5, 0.6 and 0.8 (see dotted lines on figure 5). Looking at
 144 the pressure ramp in its entirety shows a possible order of the regimes when increasing
 145 the blowing pressure: standard and double two-step motions, second register, and inverted

146 double then inverted two-step motions. Note that in this ramp, the episode between 1 and 2
 147 seconds with a closure ratio of little above 0.25 is actually a quasi-periodic oscillation, with
 148 the actual double two-step oscillation starting at around 2.3 seconds.

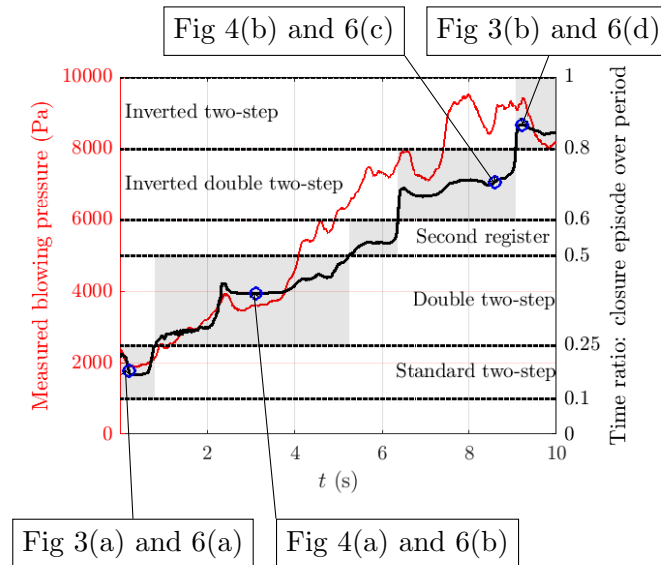


FIG. 5. Result of a blowing pressure increase (low B fingering, alto saxophone) recorded with the instrumented mouthpiece. Left y-axis (red): measured smoothed blowing pressure in Pa. Right y-axis: ratio between closure episode duration and oscillation period (solid black line), and regime separation thresholds (dotted black lines). Greyed areas emphasize the duration of each type of regime. Circles correspond to reed displacement signals in figures 3, 4 and pressure signals in figure 6.

149 **III. NUMERICAL STUDY OF THE REGIMES USING A PHYSICAL MODEL**150 **A. Saxophone model**

A simplified saxophone model consists of three main elements: the resonator, the reed channel and reed dynamics. Here all variables are dimensionless and obtained from their physical counterparts (denoted with a hat) as

$$p = \frac{\hat{p}}{p_M} \quad , \quad u = Z_c \frac{\hat{u}}{p_M} \quad , \quad x = \frac{\hat{x}}{H}, \quad (1)$$

151 where p_M is the static pressure necessary to close the reed completely, Z_c is the characteristic
 152 impedance at the input of the resonator, and H is the distance separating the reed from
 153 the mouthpiece lay at rest. Note that $x = 0$ denotes the reed at equilibrium, and $x = -1$
 154 corresponds to a closed reed channel.

155 The resonator is represented by its dimensionless input impedance, decomposed as a sum
 156 of modes

$$Z(\omega) = \frac{P(\omega)}{U(\omega)} = \sum_{n=0}^{N_m} \frac{C_n}{i\omega - s_n} + \frac{\bar{C}_n}{i\omega - \bar{s}_n}, \quad (2)$$

where C_n are the complex residues and s_n the complex poles. These modal parameters are estimated from a measured saxophone input impedance (Taillard *et al.*, 2018). Eq. (2) can be transformed into the temporal evolution of the modal components p_n , since $j\omega$ translates into a time-domain derivative by inverse Fourier transform

$$\dot{p}_n(t) = s_n p_n(t) + C_n u(t). \quad (3)$$

The acoustic pressure p at the input of the tube is expressed as a sum including the modal components

$$p(t) = 2 \sum_{n=1}^{N_m} \text{Re}(p_n(t)). \quad (4)$$

157 The number of modes N_m is chosen as $N_m = 12$, sufficiently large to represent the main
 158 resonances of the resonator. Results obtained using $N_m = 6$ lead to similar conclusions. The
 159 flow u at the input of the resonator is governed by the nonlinear characteristic (Wilson and
 160 Beavers, 1974)

$$u = \zeta[x + 1]^+ \text{sign}(\gamma - p) \sqrt{|\gamma - p|}, \quad (5)$$

where $[x + 1]^+ = \max(x + 1, 0)$. This nonlinear characteristic uses the dimensionless control parameters of reed opening at rest ζ and blowing pressure γ . The expression of these parameters are

$$\zeta = wHZ_c \sqrt{\frac{2}{\rho p_M}}, \quad \gamma = \frac{\hat{\gamma}}{p_M}, \quad (6)$$

161 where w is the effective width of the reed channel, ρ the density of air and $\hat{\gamma}$ is the physical
 162 value of the blowing pressure. For this study the parameter ζ is fixed at $\zeta = 0.6$, unless
 163 otherwise specified. Following the values of reed channel height at rest $H = 17 \times 10^{-5}$ m
 164 and reed stiffness $K = 6.4 \times 10^6$ Pa.m provided in (Muñoz Arancón *et al.*, 2016), with
 165 an approximate effective width of $w = 1.10^{-2}$ m and characteristic impedance $Z_c =$
 166 3.10^6 Pa.s/m³, one finds $\zeta = Z_c w \sqrt{2H/\rho K} = 0.58$ which justifies studying $\zeta \simeq 0.6$ in
 167 this work. To use Harmonic Balance Method and Asymptotic Numerical Method, described
 168 in subsection III B, it is convenient to regularize the characteristic of Eq. (5) using $|\cdot| \simeq$
 169 $\sqrt{\cdot^2 + \eta}$, where the parameter η is fixed at 10^{-3} (Kergomard *et al.*, 2016).

170 The reed is modeled as a single degree of freedom oscillator driven by the pressure
 171 difference between the input of the resonator and the mouth of the resonator

$$\frac{\ddot{x}}{\omega_r^2} + q_r \frac{\dot{x}}{\omega_r} + x = -(\gamma - p), \quad (7)$$

172 where ω_r and q_r are the angular frequency and damping coefficient of the reed, chosen at
 173 $\omega_r = 4224$ rad/s based on (Muñoz Arancón *et al.*, 2016) and $q_r = 1$. In this model, the
 174 impact of the reed on the mouthpiece lay is ignored (Dalmont *et al.*, 2000; Doc *et al.*, 2014).
 175 For further details on the effect of ignoring reed impact in a saxophone model, see (Colinot
 176 *et al.*, 2019).

177 B. Numerical resolution with harmonic balance method

Periodic solutions to the system of equations (2), (5) and (7) are found using the harmonic balance method (HBM), under the formalism proposed in (Cochelin and Vergez, 2009). The HBM was pioneered by (Krylov and Bogoliubov, 1949; Nakhla and Vlach, 1976), and was applied to musical instrument models first in (Gilbert *et al.*, 1989). Each variable X (where X can stand for p_n , u , x ...) is assumed to be periodic and thus decomposed into its Fourier series truncated at order H

$$X(t) = \sum_{k=-\infty}^{\infty} X_k \exp(ik\omega_0 t) \simeq \sum_{k=-H}^H X_k \exp(ik\omega_0 t), \quad (8)$$

178 where ω_0 is the angular frequency. This yield an algebraic system where the unknowns are
 179 the Fourier coefficients and the angular frequency. Hereafter, $H = 20$ is chosen, because
 180 it appears sufficient for a good representation of the studied regimes. The emergence of
 181 these different regimes depends on the value of the blowing pressure parameter γ . To

182 compare the value of γ leading to each regime to the experimental results of figure 5, a
183 Taylor-series based continuation method (Asymptotic Numerical Method) is applied to the
184 algebraic system obtained by harmonic balance (Guillot *et al.*, 2019). The source code
185 for this method may be found online at <http://manlab.lma.cnrs-mrs.fr/>. The continuation
186 yields possible periodic solutions, as well as their stability (Bentvelsen and Lazarus, 2018;
187 Lazarus and Thomas, 2010). This may be displayed as a bifurcation diagram representing
188 the evolution of one descriptor of the periodic solutions as a function of the blowing pressure.
189 The bifurcation diagrams displayed here do not change when adding more harmonics, but
190 their computation is more time consuming.

191 C. Results

192 Depending on the value of the blowing pressure parameter γ , all types of two-step regimes
193 observed experimentally are found to be stable periodic solutions of the model. Figure
194 6 compares the regime types found in measurement and simulation from their pressure
195 waveforms. No a posteriori adjustment of the model is performed, and therefore no precise
196 agreement of the waveforms is expected. Many differences between synthesized and measured
197 signals could be explained by the reed opening parameter ζ being constant and not adjusted
198 in the model, and the response of the pressure probe tube affecting the measured pressure
199 signal. Some high frequency components of synthesized signal can also be misrepresented
200 due to the modal truncation of the impedance. However, several main features of the
201 measured signals can be identified on the synthesized signals, such as the duration of the
202 short low-pressure episodes on the standard and double two-step regimes, and the short

203 high-pressure episodes on the inverted double and inverted two-step regimes. It can also
 204 be noted that both synthesized and measured signals exhibit secondary fast oscillations of
 205 small amplitude during the long episodes (open or closed). A similar “minor oscillations”
 206 phenomenon is known to appear on bowed strings (Kohut and Mathews, 1971). The opening
 207 duration of the synthesized inverted two-step regime presented in figure 6 (g) is longer than
 208 the closure duration of the synthesized standard two-step of figure 6 (a), which is contrary
 209 to the usual Helmholtz motion formulation in which both durations are determined only by
 210 the geometry of the resonator. This is always the case with the model of this paper, with
 211 both time-domain synthesis and the harmonic balance: the synthesized and standard and
 212 inverted two-step display a whole range of opening or closure durations depending on the
 213 value of the blowing pressure. This phenomenon is further detailed below, in multimedia
 214 file 5, figure 7 and the corresponding commentary.

215 The bifurcation diagram summarizing the evolution of the different oscillating regimes
 216 depending on the blowing pressure parameter γ is presented in figure 7. A parameter of the
 217 oscillating regimes, the amplitude of the first cosine – i.e., the real part of the first Fourier
 218 coefficient of Eq. (8) – of the first modal pressure p_1 is displayed. This parameter was chosen
 219 because it allows for clear separation of the branches corresponding to each regime. Note that
 220 the sign of this coefficient can be either positive or negative depending solely on a choice of
 221 phase of the oscillation. On the diagrams displayed hereafter, the sign of p_1 chosen so that the
 222 different solution branches are as easy to distinguish as possible. The most important part
 223 of the branches are stable regimes (thick lines in the figure). Each branch is labeled with the
 224 type of regime it corresponds to. The regime type is determined manually by observing the

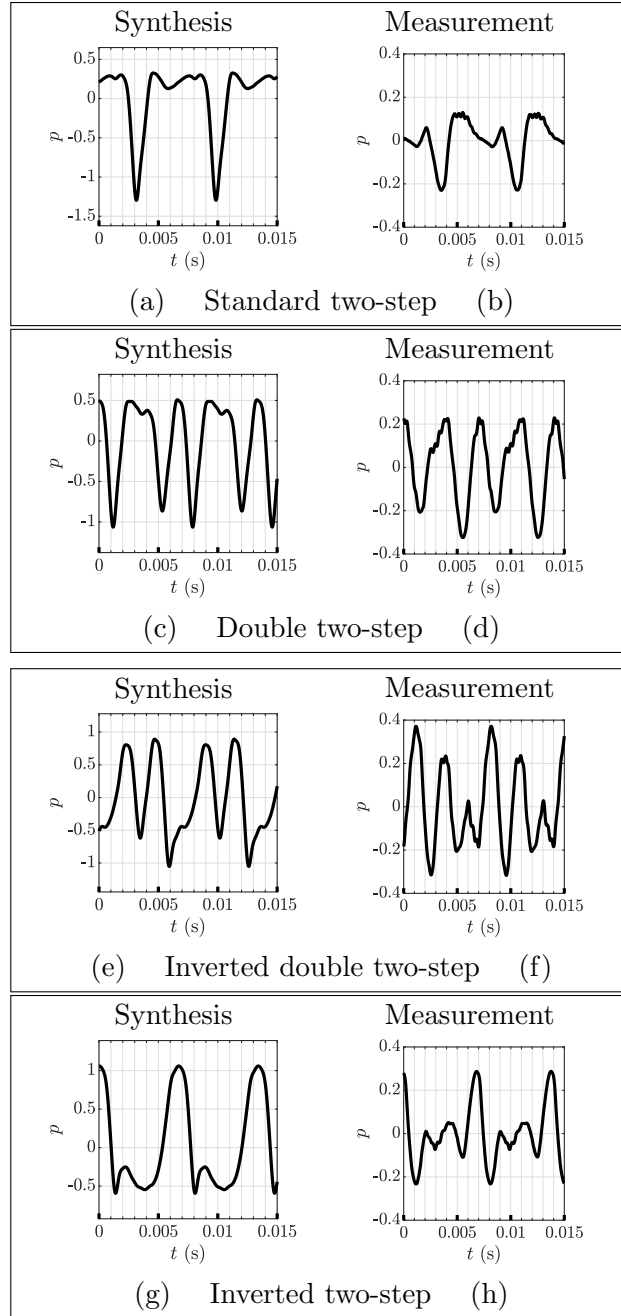


FIG. 6. Synthesized and measured pressure signals in the mouthpiece for two-step regimes.

Arbitrary units.

225 waveform, which can be done exhaustively using animations such as multimedia file 5. Note
 226 that the animation shows the standard two-step regime morphing gradually into the inverted
 227 two-step regime, on the same branch. The closure duration of the reed increases progressively

228 with the blowing pressure parameter γ , in clear contradiction with the Helmholtz motion
229 approximation. The topic of continuous transition between standard and inverted regimes
230 for a conical woodwind remains to be fully understood, although experimental explorations
231 point to similar results (Dalmont, 2007). All the other branches correspond to only one type
232 of regime each.

233 **Mm. 5.** Animation: evolution of the acoustic pressure waveform and spectrum following the
234 stable branches of the bifurcation diagram in figure 7.

235 Figure 7 is qualitatively coherent with the experimental findings in figure 5, in terms of
236 order of emergence of the stable regimes when varying the blowing pressure. Starting with
237 a low blowing pressure, the first stable regime is the standard two-step. When the blowing
238 pressure increases, the stable branch is followed until its end, and then the system jumps
239 on another stable branch. At the end of the standard two-step branch, around $\gamma = 0.69$,
240 there are two coexisting branches: the inverted two-step and the double two-step. Note
241 that for the parameter values where two stable regimes coexist, different initial conditions
242 may lead to one or the other. Describing the conditions leading to one or the other regime
243 (called their “attraction basin”) exhaustively is almost impossible. Consequently, when
244 using the bifurcation diagram to predict which regimes can be produced when increasing
245 the blowing pressure, several scenarios can be devised, and it is extremely difficult to decide
246 which one is the most probable without checking it experimentally. For instance, according
247 to this bifurcation diagram, it would be possible for the system to start from the standard
248 two-step, jump to an inverted two-step regime and follow this branch until extinction at

249 high blowing pressure ($\gamma \simeq 1.5$), with no production of double two-step regimes. However,
 250 we could not obtain this scenario experimentally. Another possible order suggested by the
 251 bifurcation diagram, after the standard two-step, is jumping to double two-step, second
 252 register, inverted double two-step, and then inverted two-step, when it is the only stable
 253 branch (for $\gamma > 1.5$). The experiment shows that it is possible to obtain all these regimes
 254 in this order of emergence when increasing the blowing pressure.

255 Figure 7 shows that the double two-step branches are linked to the second register branch:
 256 a continuum of solutions exist between second register and double two-step motion – even
 257 though some of the solutions on the path are unstable. The junction between these branches
 258 can be seen as a period-doubling of the second register. Inverted regimes appear at high
 259 blowing pressure, which is coherent with the static behavior as the reed tends to close more
 260 and more when the blowing pressure is higher. During the oscillation, the reed closes for a
 261 longer and longer portion of the period, thus transitioning from standard to inverted motion.
 262 A high blowing pressure leads to extinction of the oscillation: the reed channel stays closed.
 263 Figure 7 (b) shows the same metric as figure 5, the duration ratio between closure episode
 264 and period. It can be noted that the thresholds between the different regimes are not the
 265 same as those fixed empirically. Additionnaly, the model predicts that inverted two-step can
 266 appear at relatively low closure ratios, but these were never found experimentally. This may
 267 be due to the inverted double two-step being very stable in this blowing pressure regions,
 268 thus making it hard to find other solutions.

269 It is worth noting that the same oscillating regimes appear in the same order for other
 270 values of the reed opening parameter ζ , around the one used in figure 7 ($\zeta = 0.6$). Figure 8

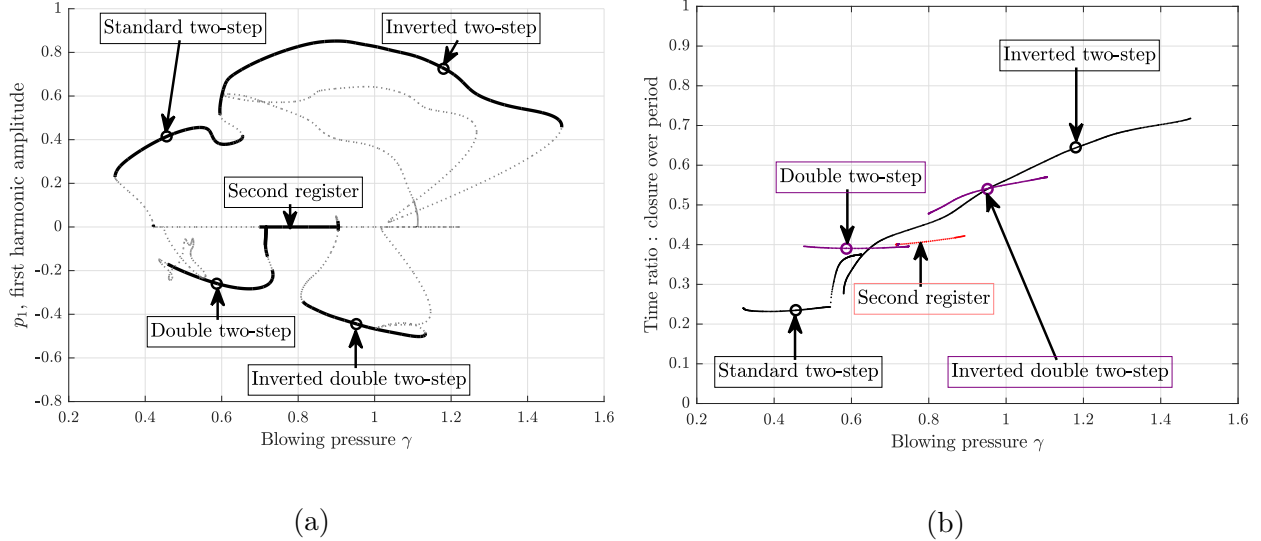


FIG. 7. Bifurcation diagram: (a) amplitude of the first cosine of the first modal pressure p_1 and (b) ratio between closure episode duration and oscillation period ; with respect to the blowing pressure parameter γ , for the low B fingering of an alto saxophone. In (a), the line aspect denotes stability of the regimes: thick black is stable, dotted gray is unstable. Circle markers correspond to the plots in figure 6. $\zeta = 0.6$.

271 shows two bifurcation diagrams, obtained for $\zeta = 0.5$ and $\zeta = 0.75$ respectively. The stability
 272 region of the regimes are affected by the value of ζ . In particular, a lower ζ enlarges the
 273 zone of stability of the second register while a greater ζ reduces it. It can also be noted
 274 that in this particular case, a higher ζ value leads to a uninterrupted single two-step branch,
 275 where standard and inverted two-step are connected by stable regimes. Another comment
 276 can be made on the bifurcation diagram obtained for $\zeta = 0.5$ (Figure 8 (a)), on the inverted
 277 double two-step branch. In this case, the inverted double-two-step branch that is connected
 278 to the second register branch only contains unstable regimes – on figure 8 (a) it is the small
 279 branch of negative p_1 , between $\gamma = 0.86$ and $\gamma = 1.04$. This branch corresponds to the
 280 branch in figure 7 where the inverted double two-step becomes stable. However, on figure 8

281 (a), another inverted double two-step branch shows stable regimes, that are indicated by the
 282 inverted double two-step arrow. This other branch is not connected to the second register,
 283 but to the inverted single two-step branch, by a long unstable portion of branch. Therefore
 284 it appears that double two-step regimes can be considered as degenerate from the single
 285 two-step or the second register, depending on the value of the control parameters.

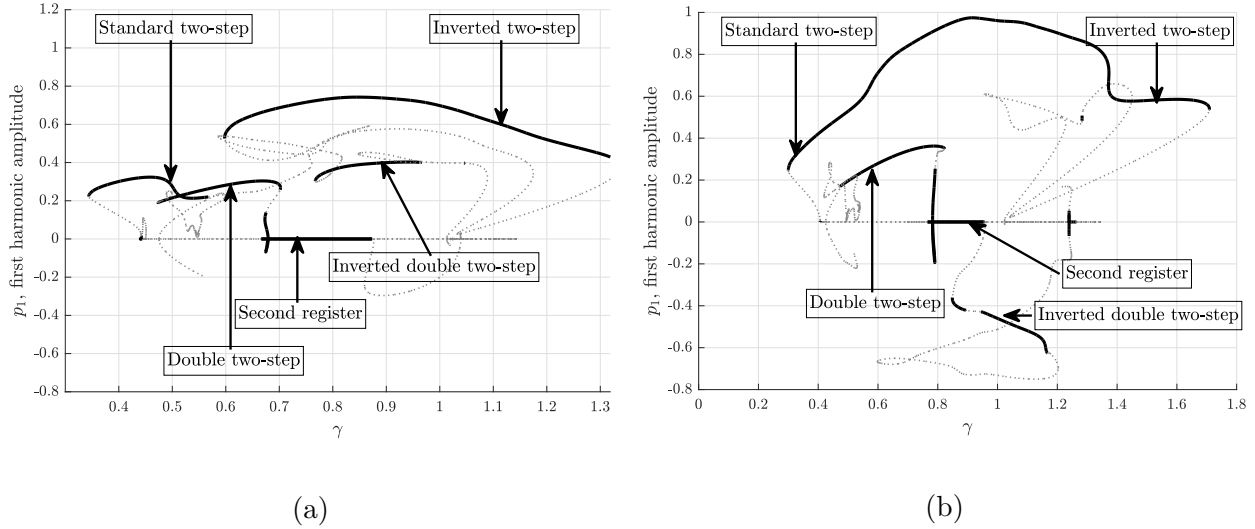


FIG. 8. Bifurcation diagram: amplitude of the first cosine of the first modal pressure p_1 with respect to the blowing pressure parameter γ , for the low B fingering of an alto saxophone. (a) $\zeta = 0.5$, (b) $\zeta = 0.75$. The line aspect denotes stability of the regimes: thick black is stable, dotted gray is unstable

286 A similar behavior is also observed for neighboring fingerings. Figure 9 shows the
 287 bifurcation diagram for the fingering just above the one used for figures 7 and 8: the low C
 288 fingering. The bifurcation diagram in figure 9 has the same structure as the others, although
 289 the inverted double two-step regime is unstable. In particular, the transition between
 290 standard two-step and inverted two-step regimes is an unstable portion of branch featuring
 291 two fold bifurcations (two points where two solutions collide and disappear, which can be

292 seen as turning-up points on the bifurcation diagram), similar to that of figure 8, up, and
 293 figure 7. It is also worth noting that on this fingering, the double two-step branch and second
 294 register branch are connected by stable regimes only: the thick lines connect at $\gamma = 0.8$.
 295 This indicates that for this fingering, it is possible to have continuous transition between
 296 double two-step and second register using only stable regimes. A synthesized example of
 297 this transition is shown in multimedia file 6.

298 **Mm. 6.** Animation: evolution of the acoustic pressure waveform and spectrum during a
 299 continuous transition between double two-step regime and second register for the low C
 300 fingering of an alto saxophone, following branches of the bifurcation diagram in figure 9.

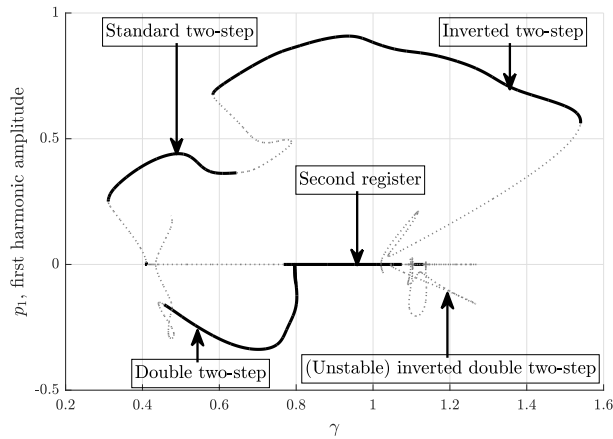


FIG. 9. Bifurcation diagram: amplitude of the first cosine of the first modal pressure p_1 with respect to the blowing pressure parameter γ , for the low C fingering of an alto saxophone. $\zeta = 0.6$, same as in figure 7.

301 The double two-step regime becomes unstable on fingerings D and higher for the main
 302 value of $\zeta = 0.6$ studied here. This may be a sign that its production is linked to the high

303 amplitude of the second and third resonances of the resonator, which is a characteristic of
304 the low fingerings of the saxophone.

305 **IV. CONCLUSION**

306 Alto saxophones are able to produce double two-steps motions, that seem analogous to
307 double stick-slip motions in bowed strings ([Woodhouse, 2014](#)). The production region of
308 these regimes appears linked to the second register of the resonator. The appearance of
309 the many oscillating regimes on the studied fingerings may be due to the strong role of
310 the second and third mode of the resonator. The simple saxophone model used in this
311 paper is capable of reproducing these regimes, even though it ignores the impact between
312 the reed and the mouthpiece lay. The model also corroborates the order of appearance of
313 these regimes when increasing the blowing pressure on a real saxophone. Complementary
314 numerical studies show that the double two-step phenomenon is not restricted to a particular
315 set of parameters, but appears for several combinations of control parameters and several
316 fingerings. The description of the playability of a saxophone in the low fingerings may
317 take these regimes into account, whether they are undesirable, as is the case for the double
318 fly-back motion in violins, or a useful tool of expressivity for the musician. Acoustical or
319 geometrical characteristics of the resonator remain to be linked to the ease of production of
320 double two-step regimes.

321 **ACKNOWLEDGMENTS**

322 The authors would like to thank Louis Guillot for advice and guidance in the construction
 323 of the bifurcation diagram. This work has been carried out in the framework of the
 324 Labex MEC (ANR-10-LABX-0092) and of the A*MIDEX project (ANR-11-IDEX-0001-
 325 02), funded by the Investissements d’Avenir French Government program managed by the
 326 French National Research Agency (ANR). This study has been supported by the French
 327 ANR 659 LabCom LIAMFI (ANR-16-LCV2-007-01).

328

329 Bentvelsen, B., and Lazarus, A. (2018). “Modal and stability analysis of structures in
 330 periodic elastic states: application to the ziegler column,” *Nonlinear Dynamics* **91**(2),
 331 1349–1370.

332 Chen, J.-M., Smith, J., and Wolfe, J. (2009). “Saxophone acoustics: introducing a
 333 compendium of impedance and sound spectra,” *Acoustics Australia* **37**(1-19).

334 Cochelin, B., and Vergez, C. (2009). “A high order purely frequency-based harmonic balance
 335 formulation for continuation of periodic solutions,” *Journal of sound and vibration* **324**(1-
 336 2), 243–262.

337 Colinot, T., Guillot, L., Vergez, C., Guillemain, P., Doc, J.-B., and Cochelin, B. (2019).
 338 “Influence of the “ghost reed” simplification on the bifurcation diagram of a saxophone
 339 model,” *Acta Acustica united with Acustica* [**In press**](–), –.

- 340 Dalmont, J.-P. (2007). “Analytical and experimental investigation of the dynamic range
341 of conical reed instruments,” in *Proceedings of the International Symposium on Musical*
342 *Acoustics, Barcelona, Spain*.
- 343 Dalmont, J.-P., Gilbert, J., and Kergomard, J. (2000). “Reed instruments, from small to
344 large amplitude periodic oscillations and the Helmholtz motion analogy,” *Acta Acustica*
345 *united with Acustica* **86**(4), 671–684.
- 346 Dalmont, J.-P., and Le Roux, J. C. (2008). “A new impedance sensor for wind instruments,”
347 *The journal of the Acoustical Society of America* **123**(5), 3014–3014.
- 348 Dalmont, J.-P., and Le Vey, G. (2014). “The irish uilleann pipe: a story of lore, hell and
349 hard d,” in *International Symposium on Musical Acoustics*.
- 350 Doc, J.-B., Vergez, C., and Missoum, S. (2014). “A minimal model of a single-reed
351 instrument producing quasi-periodic sounds,” *Acta Acustica united with Acustica* **100**(3),
352 543–554.
- 353 Gilbert, J., Kergomard, J., and Ngoya, E. (1989). “Calculation of the steady-state
354 oscillations of a clarinet using the harmonic balance technique,” *The journal of the*
355 *Acoustical Society of America* **86**(1), 35–41.
- 356 Guillemain, P., Vergez, C., Ferrand, D., and Farcy, A. (2010). “An instrumented saxophone
357 mouthpiece and its use to understand how an experienced musician plays,” *Acta Acustica*
358 *united with Acustica* **96**(4), 622–634.
- 359 Guillot, L., Cochelin, B., and Vergez, C. (2019). “A taylor series-based continuation method
360 for solutions of dynamical systems,” *Nonlinear Dynamics* 1–19.

- 361 Keefe, D. H. (1984). “Acoustical wave propagation in cylindrical ducts: Transmission line
362 parameter approximations for isothermal and nonisothermal boundary conditions,” The
363 Journal of the Acoustical Society of America **75**(1), 58–62.
- 364 Kergomard, J., Guillemain, P., Silva, F., and Karkar, S. (2016). “Idealized digital models
365 for conical reed instruments, with focus on the internal pressure waveform,” The Journal
366 of the Acoustical Society of America **139**(2), 927–937.
- 367 Kohut, J., and Mathews, M. (1971). “Study of motion of a bowed violin string,” The Journal
368 of the Acoustical Society of America **49**(2B), 532–537.
- 369 Krylov, N. M., and Bogoliubov, N. N. (1949). *Introduction to non-linear mechanics*
370 (Princeton University Press).
- 371 Lazarus, A., and Thomas, O. (2010). “A harmonic-based method for computing the stability
372 of periodic solutions of dynamical systems,” *Comptes Rendus Mécanique* **338**(9), 510–517.
- 373 Muñoz Arancón, A., Gazengel, B., Dalmont, J.-P., and Conan, E. (2016). “Estimation
374 of saxophone reed parameters during playing,” The Journal of the Acoustical Society of
375 America **139**(5), 2754–2765.
- 376 Nakhla, M., and Vlach, J. (1976). “A piecewise harmonic balance technique for
377 determination of periodic response of nonlinear systems,” *IEEE Transactions on Circuits*
378 *and Systems* **23**(2), 85–91.
- 379 Ollivier, S., Dalmont, J.-P., and Kergomard, J. (2004). “Idealized models of reed woodwinds.
380 Part I: Analogy with the bowed string,” *Acta acustica united with acustica* **90**(6), 1192–
381 1203.

- 382 Ollivier, S., Kergomard, J., and Dalmont, J.-P. (2005). “Idealized models of reed woodwinds.
383 Part II: On the stability of ”two-step” oscillations,” *Acta acustica united with acustica*
384 **91**(1), 166–179.
- 385 Pàmies-Vilà, M., Hofmann, A., and Chatziioannou, V. (2018). “Analysis of tonguing and
386 blowing actions during clarinet performance,” *Frontiers in psychology* **9**.
- 387 Schelleng, J. C. (1973). “The bowed string and the player,” *The Journal of the Acoustical*
388 *Society of America* **53**(1), 26–41.
- 389 Taillard, P.-A., Silva, F., Guillemain, P., and Kergomard, J. (2018). “Modal analysis of the
390 input impedance of wind instruments. application to the sound synthesis of a clarinet,”
391 *Applied Acoustics* **141**, 271–280.
- 392 Wilson, T. A., and Beavers, G. S. (1974). “Operating modes of the clarinet,” *The Journal*
393 *of the Acoustical Society of America* **56**(2), 653–658.
- 394 Woodhouse, J. (2014). “The acoustics of the violin: a review,” *Reports on Progress in*
395 *Physics* **77**(11), 115901.